Cancer Research

The SIRT1/HIF-2α axis drives reductive glutamine metabolism under chronic acidosis and alters tumor response to therapy

Cyril Corbet, Nihed Draoui, Florence Polet, et al.

Cancer Res Published OnlineFirst August 1, 2014.

The SIRT1/HIF-2α axis drives reductive glutamine metabolism under chronic acidosis and alters tumor response to therapy.

Cyril Corbet[1], Nihed Draoui[1], Florence Polet[1], Adan Pinto[1], Xavier Drozak[2], Olivier Riant[2] & Olivier Feron[1]

[1]Pole of Pharmacology and Therapeutics (FATH), Institut de Recherche Expérimentale et Clinique (IREC) UCLouvain, 53 Avenue E. Mounier, B-1200 Brussels, Belgium
[2]Molecules, Solids and Reactivity (MOST), Institute of Condensed Matter and Nanosciences (IMCN), UCLouvain, 1 Place Louis Pasteur, B-1348 Louvain-la-Neuve, Belgium

Running title: Acidosis-triggered reprogramming of tumor metabolism

Keywords: acidosis, cancer, metabolism, glutamine, SIRT1

Financial support: This work was supported by grants from the Fonds national de la Recherche Scientifique (FRS-FNRS), the Belgian Foundation against cancer, the J. Maisin Foundation, the interuniversity attraction pole (IUAP) research program #UP7-03 from the Belgian Science Policy Office (Belspo) and an Action de Recherche Concertée (ARC 14/19).

Corresponding author: Prof. Olivier Feron, Pole of Pharmacology and Therapeutics (FATH), Institut de Recherche Expérimentale et Clinique (IREC), UCLouvain, 53 avenue E. Mounier, B1.53.09, B-1200 Brussels, Belgium. Phone: +32-2-7645264; Fax: +32-2-7645269; E-mail: olivier.feron@uclouvain.be

Conflicts of Interest: None

Abstract: 150 words
Word count: 4802 (+ 36 references)

ABSTRACT

Extracellular tumor acidosis largely results from an exacerbated glycolytic flux in cancer and cancer-associated cells. Conversely, little is known on how tumor cells adapt their metabolism to acidosis. Here, we demonstrate that long-term exposure of cancer cells to acidic pH leads to a metabolic reprogramming towards glutamine metabolism. This switch is triggered by the need to reduce the production of protons from glycolysis and further maintained by the NAD^+-dependent increase in SIRT1 deacetylase activity to ensure intracellular pH homeostasis. Consecutive increase in HIF-2α activity promotes the expression of various transporters and enzymes supporting the reductive and oxidative glutamine metabolism whereas a reduction in functional HIF-1α expression consolidates the inhibition of glycolysis. Finally, *in vitro* and *in vivo* experiments document that acidosis accounts for a net increase in tumor sensitivity to inhibitors of SIRT1 and glutaminase GLS1. These findings highlight the influence that tumor acidosis and metabolism exert on each other.

INTRODUCTION

Acidosis and cycling hypoxia are two well-known physico-chemical properties of the tumor microenvironment (1, 2). The release of lactate (the end-product of glycolysis) together with a proton by hypoxic tumor cells but also the hydratation of CO_2 into bicarbonate and proton (by tumor cells that have access to O_2) contribute to the acidification of the tumor microenvironment. Large amounts of lactate/H^+ are also released by tumor cells exhibiting aerobic glycolysis (the so-called Warburg effect) (3, 4). Extracellular pH (pHe) has actually been determined in a wide variety of cancers to be significantly more acidic than in normal tissues, with values ranging from 5.9 to 7.2 (5, 6). Acidosis is known to contribute to the genetic instability of tumor cells (7) and to profoundly alter their transcriptomic profile (8) leading to phenotypes that are particularly suited for survival and growth in an acidic environment. A low pHe has for instance a wide impact on cancer progression by promoting tumor cell migration, invasion and metastasis (9-11) and by stimulating angiogenesis (12-14). Although tumor metabolic peculiarities directly account for the acidification of the tumor microenvironment, whether acidosis may itself influence metabolism remains elusive. One may however reason that when the extracellular acidic stress increases or persists, reducing the source of H^+ by shifting the metabolic preference may also represent an option for tumor cells. Interestingly, while glucose metabolism is generally viewed as the main contributor to acidic tumor pHe, glutamine metabolism is less prone to H^+ production. Glutamine can for instance support anaplerosis/cataplerosis without the need for TCA cycle to be coupled to OXPHOS and may thus supply tumor cells with ATP as well as a large variety of biosynthetic precursors and redox equivalents without producing carbonic acid (15-17).

Although a few studies have addressed the effects of acute changes in pHe on tumor metabolism (8, 18), interpretation is usually complicated by the overall tumor cell death

associated with the rapid exposure of tumor cells to an acidic pH. In this study, we postulated that long-term selection of tumor cells able to survive and proliferate under acidic conditions could offer more relevant models to get insights on the influence of acidosis on tumor metabolism. We found that despite a similar proliferation rate in tumor cells adapted to acidic pH and in parental cells (maintained at pH 7.4), a metabolic shift from a largely glycolytic metabolism towards the reductive glutamine metabolism was actually observed in response to chronic acidic conditions. The capacity of different tumor cells to develop a resistance to the intracellular acidification was associated with an increase in SIRT1-driven protein deacetylation leading to a reduction in HIF-1α activity and abundance concomitantly to a net increase in HIF-2α activity and expression. Major targets of the latter were identified including the glutamine transporter SLC1A5 and the glutaminase isoform GLS1, both supporting the preferential glutamine metabolism and a corresponding shift in the response to therapeutic interventions.

MATERIALS AND METHODS

Cell culture

All cell lines were acquired in the last three years from ATCC where they are regularly authenticated by short tandem repeat profiling. Cells were stored according to the supplier's instructions and used within 6 months after resuscitation of frozen aliquots. SiHa cervix cancer cells, FaDu pharynx squamous cell carcinoma cells and HCT-116 colon cancer cells were maintained in DMEM supplemented with 25 mM of both PIPES and HEPES to adjust pH to 7.4 or 6.5.

Transfection

Tumor cells were transfected with 50 nM siRNA using Lipofectamine™ RNAiMAX (Life Technologies). Sequences are described in Supplementary Data. Plasmids encoding Flag-tagged wild-type or mutant H363Y SIRT1 were obtained from Addgene and were transfected with Lipofectamine 2000 (Life Technologies).

Metabolic profiling

Cells were cultured for 24h in DMEM supplemented with either 10 mM D-[U-^{13}C]glucose and 2 mM unlabeled L-glutamine, or 10 mM unlabeled D-glucose and 2 mM L-[U-^{13}C]glutamine (CLM-1822, Cambridge Isotope Laboratories). Mass spectrometry measurements were performed by the University of Michigan Metabolomics Resource Core (19). Glucose and lactate concentrations were measured using enzymatic assays (CMA Microdialysis AB) and a CMA 600 analyzer (Aurora Borealis). Glutamine concentration was determined with a colorimetric assay from BioAssay Systems. Intracellular NAD^+ and NADH contents were determined by using a dedicated quantification kit (Sigma-Aldrich). To measure amino acid uptake, SiHa cells were incubated at 37°C in a Krebs solution containing either 2 µM L-glutamine + L-[^{3}H]-glutamine or 0.8 µM L-leucine + L-[^{3}H]-leucine;

radioactivity was determined in a microplate counter (PerkinElmer Topcount). Oxygen-consumption rate (OCR) and extracellular-acidification rate (ECAR) were measured using the Seahorse XF96 plate reader.

Western blot analysis

Immunoprecipitation and Western blotting experiments were carried out as reported elsewhere (20); antibodies are listed in Supplementary Data.

Intracellular pH measurements

Cells were loaded with the pH-sensitive dye carboxy-SNARF-1-AM for 30 min. After washing, cells were exposed to media buffered at pH 7.4 or 6.5, and SNARF-1 fluorescence was recorded at 580 and 642 nm after excitation at 485 nm, in a Victor X4 fluorescence microplate reader (PerkinElmer).

***In vivo* experiments**

All the experiments involving mice received the approval of the university ethic committee (approval ID 2012/UCL/MD005) and were carried out according to national animal care regulations. Seven week-old female NMRI nude mice were purchased from Elevage Janvier and $2x10^6$ native tumor cells (pH 7.4) or pH 6.5-adapted tumor cells were injected subcutaneously in the left and right flanks, respectively. When tumors reached a mean diameter of 5 mm, BPTES (10 $mg.kg^{-1}$) or EX-527 (2 $mg.kg^{-1}$) were daily injected intraperitoneally.

Statistical analysis

Results are expressed as mean ± SEM of at least three independent experiments. Two-tailed unpaired Student t-test, one-way or two-way ANOVA tests (Bonferroni's post-hoc test) were used where appropriate.

RESULTS

Chronic acidosis causes a shift from glucose to glutamine metabolism in three different tumor cell lines.

To study the metabolic adaptation of cancer cells to an acidic environment, we cultured several tumor cell lines in a medium buffered at pH 6.5. We first observed that a 72h-incubation in the acidic medium led to a significant inhibition of tumor cell growth (see 6.5/acute condition in Fig. 1A). We then maintained tumor cells in this medium (repeatedly renewed) for 8-10 weeks till they completely recovered and grew at the same rate as parental cells (see 6.5 *vs* 7.4 conditions in Fig. 1A). We carried out this procedure on three different cell lines, namely SiHa, FaDu and HCT-116 cancer cells, with similar results (Fig. 1A).

We then investigated possible changes in the consumption of either glucose or glutamine in tumor cells adapted to acidic pH 6.5 (called 6.5/tumor cells here below) *vs* parental cells maintained at pH 7.4 (*i.e.* 7.4/tumor cells). Interestingly, glutamine consumption was increased (Fig. 1B) while glucose consumption and lactate secretion were dramatically reduced (Figs 1C and 1D) in the three cell lines chronically cultured at pH 6.5 (see also Figs S1A-C). Preference for glutamine over glucose for 6.5/tumor cells was confirmed by culturing tumor cells in media deprived of either fuel: glutamine deprivation significantly reduced the growth of the three 6.5/tumor cell lines whereas glucose deprivation was more detrimental for the corresponding parental 7.4/tumor cells (Fig. 1E and Fig. S1D). Similarly, inhibition of glucose metabolism by 2-deoxyglucose (2-DG) reduced parental cell growth, by about 50%, while it did not or barely affect the growth of 6.5/tumor cells (Fig. 1F and Fig. S1E). Conversely, inhibition of glutamine metabolism by using L-γ-glutamyl-p-nitroanilide (GPNA), an inhibitor of SLC1A5 (ASCT2), the main glutamine transporter in carcinoma cells (21, 22) or by using BPTES, a glutaminase (GLS1)-selective inhibitor (23) reduced the growth of 6.5/tumor cells compared to parental cells (Fig. 1F and Fig. S1E).

Chronic acidosis enhances both glutamine-fueled respiration and reductive glutamine metabolism.

Using radiolabelled glutamine, we then confirmed that SiHa/6.5 cells displayed a significantly higher rate of glutamine uptake than parental cells (Fig. 2A). Immunoblotting experiments also showed that the expression of both SLC1A5 and GLS1 was significantly increased ($P < 0.01$, n=3) (Fig. 2B); expression of glutaminase GLS2 and glutamine synthetase GS was not altered (Fig. 2B). Inhibition of SLC1A5 expression by gene silencing reduced SiHa/6.5 cell growth by about 50% whereas a limited 20% reduction was found in SiHa/7.4 (Fig. 2C), confirming the results with the pharmacological inhibitor of glutamine influx, GPNA (Fig. 1F).

We also found that SiHa/6.5 cells exhibited higher oxygen consumption rate (OCR) at basal level but also after exposure to glutamine (*vs* SiHa/7.4 cells) (Fig. 2D); both basal and stimulated OCR were inhibited by mitochondrial respiratory chain inhibitors, rotenone and antimycin A (Fig. 2D). We also found that DM-αKG, a cell-permeable analog of α-ketoglutarate, could partially restore the extent of SiHa/6.5 cell growth to the level observed in the presence of glutamine (Fig. 2E).

We also incubated cells with [U^{13}-C_5]glutamine and analyzed the incorporation in various metabolites using gas chromatography-mass spectrometry. We found that SiHa/6.5 displayed an increase in reductive glutamine metabolism (Fig. 2F), as documented by increases in the m+3 mass isotopomers of malate and fumarate (Fig. 2G) and in the m+5 mass isotopomer of citrate (*vs* m+4 citrate) (Fig. 2G and 2H). Interestingly, we also found that isocitrate dehydrogenase-1 (IDH1), the enzyme identified as the main support to glutamine reductive carboxylation (24), was overexpressed in SiHa/6.5 (Fig. 2I). Also, IDH1 gene silencing strongly inhibited the growth of SiHa/6.5 while it did not affect SiHa/7.4 cells (Fig. 2J).

We finally examined the glutamine-dependent capture of major amino acids (25). We found that leucine uptake was increased in SiHa/6.5 (Fig. S2A). Also, knocking down the expression of SLC7A5, one of the two subunits composing the large neutral amino acids transporter LAT1, significantly reduced the growth of SiHa/6.5 but not of SiHa/7.4 cells (Fig. S2B).

Glycolysis inhibition only partly mimics acidosis-triggered increase in glutamine metabolism.

Using [U^{13}-C_6]glucose to probe glucose fate (Fig. 3A), we also showed that the glycolytic flux was strongly reduced in SiHa/6.5 as documented by a decrease in the m+3 mass isotopomers of pyruvate and lactate (Fig. 3B), confirming the data obtained in Fig.1D. Reduced glucose uptake in SiHa/6.5 cells also affected oxidative metabolism, as m+2 mass isotopomers of glucose-derived TCA cycle intermediates including α-ketoglutarate, succinate or malate were decreased (Fig. S3A). Moreover, the contribution of glucose to cell respiration was significantly reduced in SiHa/6.5 cells despite a basal increase in OCR (Fig. S3B). Interestingly, we observed a concomitant decrease in the expression of the glucose transporter GLUT1 and the monocarboxylate transporter MCT4, known to mediate glucose uptake and lactate release, respectively (Fig. 3C).

We then determined if glycolysis inhibition was the trigger of the enhanced glutaminolysis observed in acidic conditions. To address this question, we exposed SiHa cells to the glycolysis inhibitor 2-DG for several weeks in order to isolate tumor cells independent of glucose uptake for growth (SiHa/2-DGR) (Fig. 3D). We could document in SiHa/2-DGR cells, a decrease in ECAR, at basal level, but also after glucose treatment, as for SiHa/6.5 cells (Fig. 3E). Of note, an almost complete inhibition of both lactate release and glucose consumption was observed (Fig. S3C), indicating that there was no major derivation of glucose towards other pathways. SiHa/2-DGR cells also exhibited an increase in glutamine

consumption (*vs* SiHa/7.4) although to a lower extent (P<0.001) than SiHa/6.5 cells (Fig. 3F). When SiHa/2-DGR cells were placed at pH 6.5, however, glutamine consumption reached a similar level to that observed in SiHa/6.5 (Fig. 3F).

MCT1 and SIRT1 contribute to the maintenance of the intracellular pH in tumor cells chronically exposed to acidosis.

Interestingly, we observed that control SiHa/7.4 cells placed in a medium buffered at pH 6.5 exhibited a rapid and prolonged decrease in intracellular pH (Fig. 4A). By contrast, when SiHa/6.5 cells were transferred from a medium at pH 7.4 to pH 6.5, they rapidly recovered from the initial pH fall to a neutral and even slightly alkaline pH (Fig. 4A).

Among the variety of mechanisms to maintain pHi in response to changes in pH_e, MCTs have been shown to play key roles particularly at low pH_e values (26-28). Since we showed that MCT4 expression was reduced at pH 6.5, we examined the expression of MCT1, a more ubiquitous MCT isoform supporting transport of H^+/lactate and ketone bodies. We found that MCT1 was significantly more abundant in SiHa/6.5 cells together with c-myc, a recently elicited trigger of MCT1 expression (29) (Fig. 4B). Furthermore, silencing MCT1 reduced the growth of SiHa/6.5 cells up to 30% whereas this treatment had no effect in SiHa/7.4 cells (Fig. 4C). Interestingly, accumulation of ketones was detected in the extracellular medium of cultured SiHa/6.5 cells (Fig. 4D), supporting the hypothesis that acetate could be the counteranion co-transported with H^+ through MCT1. Indeed, a recent study reported that the dynamic acetylation and deacetylation of histones together with flux of acetate anions and protons in and out of the cell through the MCTs provided a mechanism for cells to modulate their pH_i (30). We reasoned that among the different histone deacetylases, the NAD^+-dependent sirtuins were the most likely to be involved in this regulation since in parallel, we showed that NAD^+ concentration was significantly increased in SiHa/6.5 cells (*vs* SiHa/7.4)

(Fig. 4E) but also in FaDu/6.5 and HCT-116/6.5 cells (Fig. S4A). We next examined the effects of siRNA targeting MCT1 as well as SIRT1, the major stress-sensitive NAD^+-dependent protein deacetylase, on the rate of pH recovery of SiHa/6.5 cells when transferred from pH 7.4 to 6.5. We found that both treatments prevented the restoration of pHi (*vs* sham SiHa/6.5 cells) (Fig. 4F).

SIRT1 supports the adaptation of tumor cells to chronic acidosis through changes in HIF-1α and HIF-2α acetylation and abundance.

To further validate the role of SIRT1, we first showed that EX-527, a cell-permeable, selective inhibitor of SIRT1 (31) inhibited the growth of SiHa/6.5 but not of SiHa/7.4 cells (Fig. 5A) and that overexpression of a deacetylase-defective mutant of SIRT1 (H363Y) acting as a dominant-negative protein led to similar results (Fig. 5B). We then performed SIRT1 knockdown and knock-in experiments. We found that SIRT1 silencing blocked proliferation of SiHa/6.5 cells (Fig. 5C) and that re-expression of wild-type SIRT1 but not mutated SIRT1 (see immunoblots in Fig. 5E) restored both cell proliferation (Fig. 5C) and glutamine consumption (Fig. 5D). Similar results were obtained with FaDu/6.5 and HCT-116/6.5 cells (Fig. S4B). Restoration of the glutamine metabolism was further supported by the re-expression of GLS1 and SLC1A5 in wild-type-SIRT1 but not mutated-SIRT1 knock-in cells (Fig. 5E). Also, in these knock-in experiments, the glucose-to-lactate metabolism was found to be regulated in an opposite fashion to that of glutamine (Fig. S4C).

SIRT1 has been described to deacetylate both HIF-1α and HIF-2α, altering their activity in opposing directions (32, 33), deacetylation suppressing HIF-1α activity but promoting the activity of HIF-2α. The use of antibodies directed against acetylated lysines to probe immunoprecipitated HIF-1α and HIF-2α (see Fig. S4D and S4E) confirmed that both HIF isoforms were deacetylated in SiHa/6.5 cells (*vs.* SiHa/7.4 cells) (Figure 5F). The SIRT1

H363Y mutant (but not wild-type SIRT1) and the SIRT1 inhibitor EX-527 significantly increased the extent of HIF acetylation (Fig. S4D-E). Interestingly, although SIRT1 abundance was not modified in SiHa/6.5 and SiHa/7.4, HIF-1α expression was decreased and HIF-2α expression was increased in SiHa/6.5 (*vs* SiHa/7.4) (Figure 5G), indicating that activity but also expression of HIF could be altered in response to acidic pH. We also examined the protein levels of different cancer cell metabolism regulators, the expression of which reported to be HIF-1α or HIF-2α dependent. Using siRNA-based strategies, we found that the HIF-2α targets SLC7A5 and GLS1 were upregulated in SiHa/6.5 in a strictly HIF-2α-dependent manner (Fig. 5H). By contrast, the HIF-1α target MCT4 was downregulated in SiHa/6.5 in agreement with the decrease in HIF-1α expression observed in these cells (Fig. 5H). Finally, we found that while SiHa/7.4 cell growth was strongly dependent on HIF-1α expression (Fig. 5I), SiHa/6.5 cell growth was reduced by about 70% when HIF-2α was silenced but remained unaffected when HIF-1α was silenced (Fig. 5I).

Acidosis-triggered metabolic shift toward glutamine metabolism is reversible and parallels the opposite alterations in HIF-1α and HIF-2α abundance.

We finally explored the reversibility of the metabolic reprogramming resulting from chronic tumor cell exposure to acidic pH. SiHa/6.5 cells were cultured at pH 7.4 for 24 to 96 hours. SiHa/6.5 cells restored their original metabolism, with a progressive increase in glucose consumption (and lactate release) (Fig. 6A) and a reduction in glutamine uptake (Fig. 6B). A similar reversibility of the metabolic phenotype was observed with FaDu/6.5 and HCT-116/6.5 cells although with a much faster kinetics than in SiHa cells (Figs. S5A and S5B). Reversal to the original glucose metabolism was associated with a decrease in intracellular NAD^+ content after 48h incubation at pH 7.4 (Fig. 6C). Moreover, when SiHa/6.5 cells were cultured at pH 7.4, acetylation of both HIF-1α and HIF-2α was progressively restored, in

agreement with a decrease in NAD^+-dependent SIRT1 activity (Fig. 6D). Importantly, the abundance of HIF-1α and HIF-2α also progressively increased and decreased with the incubation time at pH 7.4, respectively, to reach basal levels similar to parental cells continuously maintained at pH 7.4 (Fig. 6D). Proteins under the control of HIF-2α including SLC1A5, MCT1 and IDH1 (see above) remarkably followed the same pattern of reduced expression while the expression of MCT4, a *bona fide* HIF-1α target, increased in parallel to the increase in HIF-1α abundance. (Fig. 6D).

Inhibition of SIRT1-driven glutamine metabolism delays the growth of tumors arising from acidic pH-adapted cancer cells.

To explore the *in vivo* relevance of the SIRT1-mediated shift in glutamine metabolism, we first looked at the effect of BPTES on the growth of SiHa/6.5 xenograft in mice; SiHa cells were chosen for these *in vivo* experiments as they exhibited the slower phenotype reversibility and were thus more prone to maintain their *in vitro* phenotype after injection (see Figs. 6A and 6B). Interestingly, daily administration of 10 $mg.kg^{-1}$ BPTES significantly reduced the growth of SiHa/6.5 tumors but not that of SiHa/7.4 tumors (Figs. 7A and 7B). We also treated SiHa tumor-bearing mice with EX-527 (2 $mg.kg^{-1}$) and found that daily treatment with this SIRT1 inhibitor also exclusively impaired SiHa/6.5 tumor growth (Fig. 7C). Interestingly, tumor xenografts derived from SiHa/6.5 cells displayed the same phenotype as observed *in vitro* (*i.e.* SLC1A5, MCT1 and IDH1 overexpression, associated with MCT4 downregulation) (Fig. 7D).

DISCUSSION

In the present study, we have characterized the metabolic reprogramming occurring in tumor cells chronically exposed to acidic pH and documented an associated shift in the sensitivity to therapeutic modalities. We used tumor cells maintained for several weeks at pH 6.5 to avoid the confusing effects of a rapid change in extracellular pH (see Figs. 1A and 4A). The chronic adaptation to acidic pH led to a cell phenotype with the exact same proliferation rate as that of parental cells maintained at pH 7.4 but exhibiting dramatic alterations in the cellular metabolic preferences. This metabolic shift was shared by tumor cells of distinct origins, thereby excluding clonal selection of cells harboring specific mutations patterns. The acidification-triggered alterations in the metabolic profile include a dramatic reduction in the use of glucose and thus in the glycolytic flux, an increase in the reductive metabolism of glutamine together with an increase in glutamine-fueled OXPHOS. Reductive metabolism of alpha-ketoglutarate (αKG) was recently reported to represent a glucose-independent manner to synthesize AcCoA for lipid synthesis in an IDH1-dependent manner (24). Although this was so far proposed to occur under hypoxia (thus in a context of OXPHOS inhibition), our data support a model where (i) glutamine-dependent reductive carboxylation occurs in the cytosol as supported by the upregulation of the cytosolic isoform IDH1 (but not the mitochondrial IDH2) and (ii) concomitantly, glutamine supports mitochondrial cell respiration through the fueling of oxidative TCA cycle. Importantly, through the identification of the mechanisms supporting this metabolic conversion toward the preferential use of glutamine, we also provide evidence that the modalities inhibiting proliferation at acidic or physiological pH are different and may thus influence the therapeutic outcomes for patients treated with drugs targeting tumor metabolism.

McBrian and colleagues (30) reported that deacetylation of chromatin functions as a rheostat to regulate pHi when cells are exposed to an acidic extracellular pH. We report here

that in addition to a global unspecific deacetylation process, the NAD^+-dependent histone deacetylase SIRT1 drives this phenomenon in an unexpected specific manner. SIRT1-mediated deacetylation of both HIF-1α and HIF-2α is actually observed in cells chronically exposed to acidic pH and accounts for a reduction in HIF-1α activity and a net increase in HIF-2α activity. While the latter promotes the expression of the glutamine transporter ASCT2 and the glutaminase enzyme GLS1, the reduction in HIF-1α activity is associated with a reduction in MCT4, the *bona fide* monocarboxylate transporter responsible for lactate/H^+ release. By contrast, MCT1, another MCT isoform is upregulated in accordance with the role of this transporter in the efflux of protons with acetate as the counteranion. Altogether these alterations in the expression of key metabolic actors resulting from deacetylation of the HIF protein family support the preferential use of glutamine and the reduced glucose metabolism in tumor cells adapted to the acidic pH environment. Interestingly, although tumor cell clones resistant to 2-DG (SiHa/2-DGR) led to a reduction in the glycolytic flux to the same extent as tumor cells adapted to acidosis (Fig. 3E), glutamine consumption was significantly less increased in SiHa/2-DGR than in SiHa/6.5 (Fig. 3F). Moreover, acidification of SiHa/2-DGR led to an increment in glutamine consumption (Fig. 3F), indicating that glycolysis inhibition alone is not sufficient to explain the metabolic shift observed in response to long-term acidosis. A model of two parallel pathways reinforcing each other can therefore be proposed (Fig. S6). From one hand, acidification of the extracellular tumor environment accounts for the blockade of lactate/H^+ efflux and thus of glycolysis (in order to limit the production of H^+), leading to an increase in NAD^+ that activates SIRT1. From the other hand, the extra pool of protons that enter the cells are handled by acetate that acts as a counteranion to transport H^+ out of the cells (Fig. S6). Altogether, the continual loss of free acetate in cells exposed to acidic pHe together with the increased activity of SIRT1 concur to influence the acetylation and thus the activity of HIF-1α and HIF-2α as emphasized above.

In our study, the regulation of either HIF isoform according to the extracellular pH conditions can be documented in terms of both acetylation and abundance. The opposite effects of HIF-1α *vs.* HIF-2α deacetylation are in adequation with previous reports. Indeed, SIRT1 was reported to form a complex with HIF-2α and to deacetylate lysine residues in the N-TAD region, leading to an increase in HIF-2α transcriptional activity (33) while similar deacetylation of lysine residues in HIF-1α was associated with the blockade of p300 recruitment and consecutive HIF-1α transcriptional repression (32). Changes in the HIF abundance were not reported in these two studies focused on the regulation of HIF activity by SIRT1 under hypoxia. In our models of cells adapted to acidic pH under normoxic conditions, the reduction in HIF-1α abundance and the elevation of the HIF-2α expression level further reinforce the opposite changes resulting from the deacetylation of either transcription factor. This mode of regulation supports a major role of HIF-2α to drive the glutamine metabolism in replacement of the preferred glucose metabolism observed at neutral pH.

In conclusion, we report here how acidosis occurring in the tumor microenvironment may dramatically influence the tumor metabolic preferences and thereby directly modulate sensitivity (and resistance) to therapeutic modalities. In particular, our data suggest that the efficacy of treatments targeting acidosis-associated metabolic pathways using inhibitors of sirtuins and glutaminase (34-36) may have been underestimated to date by using cancer cell lines poorly reflecting the status of acidic tumors.

REFERENCES

(1) Gatenby RA, Gillies RJ. A microenvironmental model of carcinogenesis. Nat Rev Cancer 2008;8:56-61.

(2) Brahimi-Horn MC, Bellot G, Pouyssegur J. Hypoxia and energetic tumour metabolism. Curr Opin Genet Dev 2011;21:67-72.

(3) Vander Heiden MG, Cantley LC, Thompson CB. Understanding the Warburg effect: the metabolic requirements of cell proliferation. Science 2009;324:1029-33.

(4) WARBURG O. On the origin of cancer cells. Science 1956;123:309-14.

(5) Kallinowski F, Vaupel P. pH distributions in spontaneous and isotransplanted rat tumours. Br J Cancer 1988;58:314-21.

(6) Schornack PA, Gillies RJ. Contributions of cell metabolism and H+ diffusion to the acidic pH of tumors. Neoplasia 2003;5:135-45.

(7) Morita T, Nagaki T, Fukuda I, Okumura K. Clastogenicity of low pH to various cultured mammalian cells. Mutat Res 1992;268:297-305.

(8) Chen JL, Lucas JE, Schroeder T, Mori S, Wu J, Nevins J, et al. The genomic analysis of lactic acidosis and acidosis response in human cancers. PLoS Genet 2008;4:e1000293.

(9) Moellering RE, Black KC, Krishnamurty C, Baggett BK, Stafford P, Rain M, et al. Acid treatment of melanoma cells selects for invasive phenotypes. Clin Exp Metastasis 2008;25:411-25.

(10) Rofstad EK, Mathiesen B, Kindem K, Galappathi K. Acidic extracellular pH promotes experimental metastasis of human melanoma cells in athymic nude mice. Cancer Res 2006;66:6699-707.

(11) Estrella V, Chen T, Lloyd M, Wojtkowiak J, Cornnell HH, Ibrahim-Hashim A, et al. Acidity generated by the tumor microenvironment drives local invasion. Cancer Res 2013;73:1524-35.

(12) Fukumura D, Xu L, Chen Y, Gohongi T, Seed B, Jain RK. Hypoxia and acidosis independently up-regulate vascular endothelial growth factor transcription in brain tumors in vivo. Cancer Res 2001;61:6020-4.

(13) Xu L, Fukumura D, Jain RK. Acidic extracellular pH induces vascular endothelial growth factor (VEGF) in human glioblastoma cells via ERK1/2 MAPK signaling pathway: mechanism of low pH-induced VEGF. J Biol Chem 2002;277:11368-74.

(14) Peppicelli S, Bianchini F, Contena C, Tombaccini D, Calorini L. Acidic pH via NF-kappaB favours VEGF-C expression in human melanoma cells. Clin Exp Metastasis 2013.

(15) Kaelin WG, Jr., Thompson CB. Q&A: Cancer: clues from cell metabolism. Nature 2010;465:562-4.

(16) DeBerardinis RJ, Cheng T. Q's next: the diverse functions of glutamine in metabolism, cell biology and cancer. Oncogene 2010;29:313-24.

(17) Wise DR, Thompson CB. Glutamine addiction: a new therapeutic target in cancer. Trends Biochem Sci 2010;35:427-33.

(18) LaMonte G, Tang X, Chen JL, Wu J, Ding CK, Keenan MM, et al. Acidosis induces reprogramming of cellular metabolism to mitigate oxidative stress. Cancer Metab 2013;1:23.

(19) Lorenz MA, Burant CF, Kennedy RT. Reducing time and increasing sensitivity in sample preparation for adherent mammalian cell metabolomics. Anal Chem 2011;83:3406-14.

(20) Vegran F, Boidot R, Michiels C, Sonveaux P, Feron O. Lactate influx through the endothelial cell monocarboxylate transporter MCT1 supports an NF-kappaB/IL-8 pathway that drives tumor angiogenesis. Cancer Res 2011;71:2550-60.

(21) Fuchs BC, Bode BP. Amino acid transporters ASCT2 and LAT1 in cancer: partners in crime? Semin Cancer Biol 2005;15:254-66.

(22) Esslinger CS, Cybulski KA, Rhoderick JF. Ngamma-aryl glutamine analogues as probes of the ASCT2 neutral amino acid transporter binding site. Bioorg Med Chem 2005;13:1111-8.

(23) Robinson MM, McBryant SJ, Tsukamoto T, Rojas C, Ferraris DV, Hamilton SK, et al. Novel mechanism of inhibition of rat kidney-type glutaminase by bis-2-(5-phenylacetamido-1,2,4-thiadiazol-2-yl)ethyl sulfide (BPTES). Biochem J 2007;406:407-14.

(24) Metallo CM, Gameiro PA, Bell EL, Mattaini KR, Yang J, Hiller K, et al. Reductive glutamine metabolism by IDH1 mediates lipogenesis under hypoxia. Nature 2012;481:380-4.

(25) Nicklin P, Bergman P, Zhang B, Triantafellow E, Wang H, Nyfeler B, et al. Bidirectional transport of amino acids regulates mTOR and autophagy. Cell 2009;136:521-34.

(26) Cardone RA, Casavola V, Reshkin SJ. The role of disturbed pH dynamics and the Na+/H+ exchanger in metastasis. Nat Rev Cancer 2005;5:786-95.

(27) Messonnier L, Kristensen M, Juel C, Denis C. Importance of pH regulation and lactate/H+ transport capacity for work production during supramaximal exercise in humans. J Appl Physiol (1985) 2007;102:1936-44.

(28) Wahl ML, Owen JA, Burd R, Herlands RA, Nogami SS, Rodeck U, et al. Regulation of intracellular pH in human melanoma: potential therapeutic implications. Mol Cancer Ther 2002;1:617-28.

(29) Doherty JR, Yang C, Scott KE, Cameron MD, Fallahi M, Li W, et al. Blocking Lactate Export by Inhibiting the Myc Target MCT1 Disables Glycolysis and Glutathione Synthesis. Cancer Res 2013.

(30) McBrian MA, Behbahan IS, Ferrari R, Su T, Huang TW, Li K, et al. Histone acetylation regulates intracellular pH. Mol Cell 2013;49:310-21.

(31) Solomon JM, Pasupuleti R, Xu L, McDonagh T, Curtis R, DiStefano PS, et al. Inhibition of SIRT1 catalytic activity increases p53 acetylation but does not alter cell survival following DNA damage. Mol Cell Biol 2006;26:28-38.

(32) Lim JH, Lee YM, Chun YS, Chen J, Kim JE, Park JW. Sirtuin 1 modulates cellular responses to hypoxia by deacetylating hypoxia-inducible factor 1alpha. Mol Cell 2010;38:864-78.

(33) Dioum EM, Chen R, Alexander MS, Zhang Q, Hogg RT, Gerard RD, et al. Regulation of hypoxia-inducible factor 2alpha signaling by the stress-responsive deacetylase sirtuin 1. Science 2009;324:1289-93.

(34) Hensley CT, Wasti AT, DeBerardinis RJ. Glutamine and cancer: cell biology, physiology, and clinical opportunities. J Clin Invest 2013;123:3678-84.

(35) Lavu S, Boss O, Elliott PJ, Lambert PD. Sirtuins--novel therapeutic targets to treat age-associated diseases. Nat Rev Drug Discov 2008;7:841-53.

(36) Polet F, Feron O. Endothelial cell metabolism and tumour angiogenesis: glucose and glutamine as essential fuels and lactate as the driving force. J Intern Med 2013;273:156-65.

FIGURE LEGENDS

Figure 1: Chronic acidosis results in a metabolic switch from glucose to glutamine utilization. (A) Proliferation of SiHa, FaDu and HCT-116 cells under acute (grey) or chronic (dashed) acidic pH conditions *vs.* neutral, physiological pH (black). **(B)** Glutamine consumption, **(C)** glucose consumption and **(D)** lactate secretion (during 24h) by parental and pH 6.5-adapted tumor cells. Cell growth after 72h-incubation **(E)** in media containing either glucose or glutamine or both fuels and **(F)** following treatment with 10 mM 2-DG, 2 mM GPNA or 10 μM BPTES. Data represent means ± SEM of three independent experiments. *P<0.05, **P<0.01, ***P<0.001.

Figure 2: **Oxidative and reductive glutamine metabolism pathways are both increased under chronic acidosis**. **(A)** [^{3}H]-glutamine 6-min uptake measured in SiHa/7.4 and SiHa/6.5 cells. **(B)** Representative immunoblotting for the indicated regulators of glutamine metabolism (n=3). **(C)** SiHa cell growth (72h) following transfection with control or SLC1A5 siRNA; silencing is validated by immunoblotting. **(D)** Oxygen consumption rate (OCR) in SiHa/7.4 and SiHa/6.5 cells under basal conditions and after treatment with 2 mM glutamine and 1 μM rotenone/antimycin A. **(E)** SiHa/6.5 cell growth after 72h-incubation in medium with or without 2 mM glutamine or with 1 mM dimethyl α-ketoglutarate (and no glutamine). **(F)** Carbon atom transition map emphasizing the reductive carboxylation of [U-$^{13}C_5$] glutamine (dashed). Relative abundance of **(G)** reductive carboxylation-specific mass isotopomers of citrate (M5), malate (M3) and fumarate (M3) and of **(H)** citrate mass isotopomers in SiHa/7.4 and SiHa/6.5 cells cultured for 24h in the presence of [U-$^{13}C_5$]glutamine. **(I)** Representative IDH1 immunoblotting (n=3). **(J)** SiHa cell growth (72h) following transfection with control or IDH1 siRNA; silencing is validated by immunoblotting. Data represent means ± SEM of three independent experiments. **P<0.01, ***P<0.001.

Figure 3: **Glycolytic pathway is inhibited under chronic low pH conditions**. (**A**) Carbon atom transition map depicting oxidation of [U-$^{13}C_6$]glucose. (**B**) Relative abundance of glycolysis-specific mass isotopomers in SiHa cells cultured for 24h in the presence of [U-$^{13}C_6$]glucose. (**C**) Representative MCT4 and GLUT1 immunoblotting (n=2). (**D**) Cell growth of parental, acidic pH-adapted and 2-DG resistant SiHa cells after 72h incubation with 10 mM 2-DG. (**E**) ECAR in SiHa cells under basal conditions and after treatment with 10 mM glucose and 10 mM 2-DG. (**F**) Glutamine consumption (during 24h) in the indicated SiHa cells; note that SiHa/2-DGR at pH 6.5 correspond to SiHa/2-DGR acutely exposed to pH 6.5. Data represent means ± SEM of three independent experiments. ns, non-significant, **P<0.01, ***P<0.001.

Figure 4: **MCT1 and SIRT1 contribute to the maintenance of the intracellular pH in tumor cells exposed to chronic acidosis**. (**A**) Intracellular pH measurements in SiHa cells incubated at pH 7.4 for 5 min and then changed to pH 6.5 for 90 min. (**B**) Representative MCT1 and c-myc immunoblotting (n=3). (**C**) SiHa cell growth (72h) following transfection with control or MCT1 siRNA; silencing is validated by immunoblotting. (**D**) Ketones measurement in conditioned medium after 72h; b.d.l.: below detection level (**E**) NAD^+ and total NAD^+/NADH contents in indicated SiHa cells. (**F**) Intracellular pH measurements in SiHa/6.5 cells following transfection with control, MCT1 or SIRT1 siRNA, incubated at pH 7.4 for 5 min and then changed to pH 6.5 for 90 min. Data represent means ± SEM of three independent experiments. ***P<0.001.

Figure 5: **Changes in both acetylation and abundance of HIF-1α and HIF-2α support the metabolic adaptation of tumor cells to chronic acidosis.** SiHa cell growth (72h) following (**A**) treatment with 1 μM SIRT1 inhibitor EX-527, (**B**) transfection with wild-type or catalytically impaired H363Y mutant SIRT1 and (**C**) transfection with control or SIRT1 siRNA alone or together with wild-type (WT) or H363Y (MUT) SIRT1 (knock-in). (**D**)

Glutamine uptake and (**E**) representative GLS1 and SLC1A5 immunoblotting in the above knock-down and knock-in conditions. (**F**) Acetylation level of HIF-1α and HIF-2α in the indicated SiHa cell populations, as derived from immunoblots in Figs. 6D and S4D-E. (**G**) Representative SIRT1, HIF-1α and HIF-2α immunoblotting (n=3). (**H**) Expression of glycolysis-associated (HIF-1α and MCT4) and glutaminolysis-associated proteins (HIF-2α, SLC7A5, GLS1) in SiHa cells following transfection with control, HIF-1α or HIF-2α siRNA. (**I**) SiHa cell growth (72h) following transfection with control, HIF-1α or HIF-2α siRNA. Immunoblot experiments were repeated 2 to 3-fold with similar results and bar graphs represent means ± SEM of three independent experiments. ns, non-significant, *P<0.05, **P<0.01, ***P<0.001.

Figure 6: Acidosis-triggered metabolic shift is reversible and parallels the opposite alterations in the abundance of HIF-1α and HIF-2α. (**A**) Glucose consumption, lactate secretion and (**B**) glutamine consumption (during 24h) by SiHa/7.4 and SiHa/6.5 incubated at pH 7.4 for the indicated time. (**C**) NAD^+ and total NAD^+/NADH contents in corresponding SiHa cells. (**D**) Immunoprecipitation experiments depicting the extent of HIF-1α and HIF-2α acetylation on lysine residues and expression of metabolism-associated proteins in corresponding SiHa cells. Immunoblot experiments were repeated 2 to 3-fold with similar results and bar graphs represent means ± SEM of three independent experiments. **P<0.01.

Figure 7: **Inhibition of SIRT1-driven glutamine metabolism delays the growth of tumor cells pre-adapted to acidic pH.** (**A**) Tumor growth of SiHa/7.4 and SiHa/6.5 xenografts in nude mice daily treated or not with BPTES (10 $mg.kg^{-1}$). (**B**) Representative pictures of corresponding excised tumors. (**C**) Tumor growth of SiHa/7.4 and SiHa/6.5 xenografts in nude mice daily treated with EX-527 (2 $mg.kg^{-1}$). (**D**) Expression of metabolism-associated proteins in three representative vehicle-treated SiHa/7.4 and SiHa/6.5 xenografts. Data represent means ± SEM of n=5-7. ns, non-significant, **P<0.01, ***P<0.001.

Figure 1

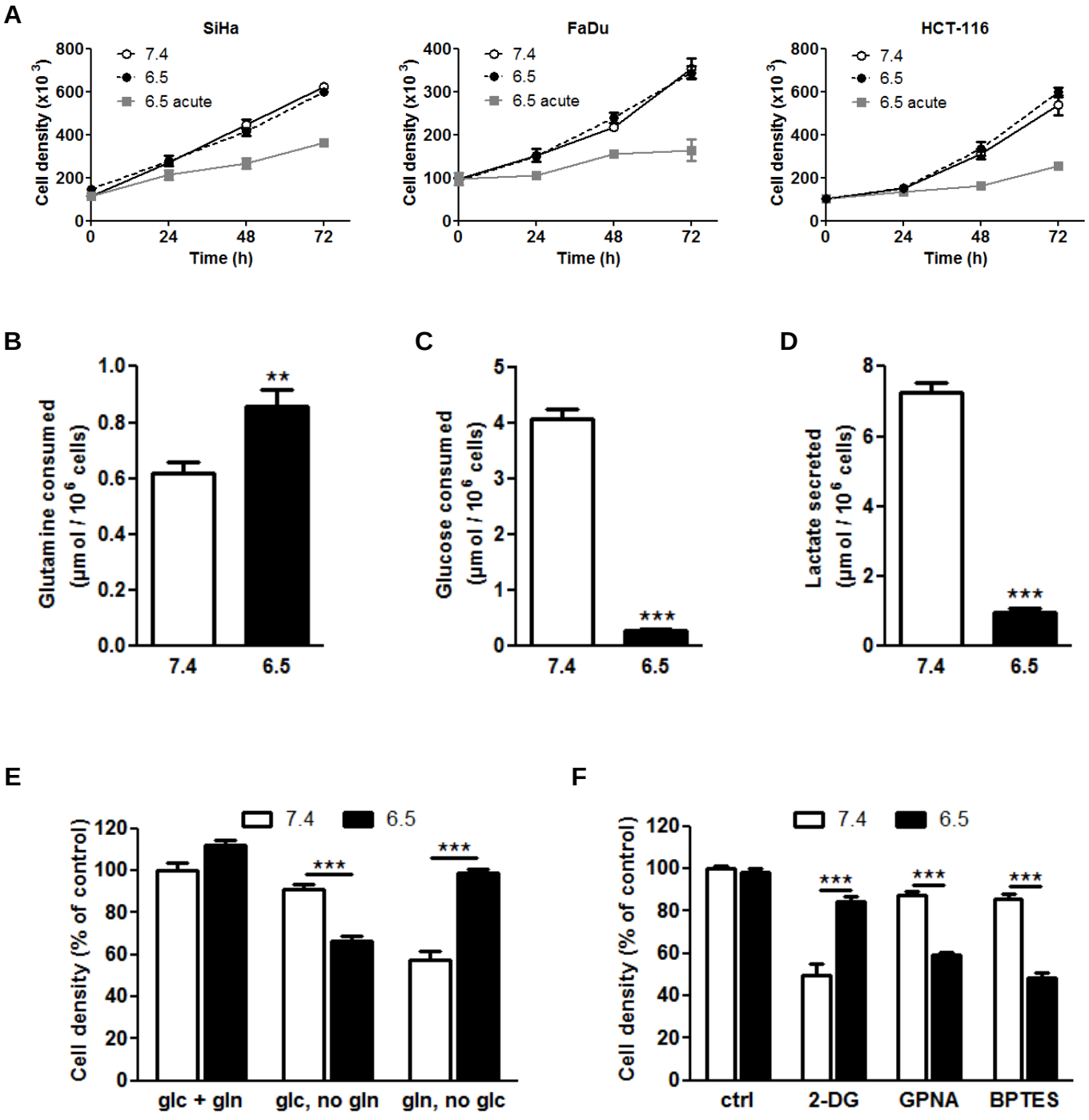

Author Manuscript Published OnlineFirst on August 1, 2014; DOI: 10.1158/0008-5472.CAN-14-0705
Author manuscripts have been peer reviewed and accepted for publication but have not yet been edited.

Figure 2

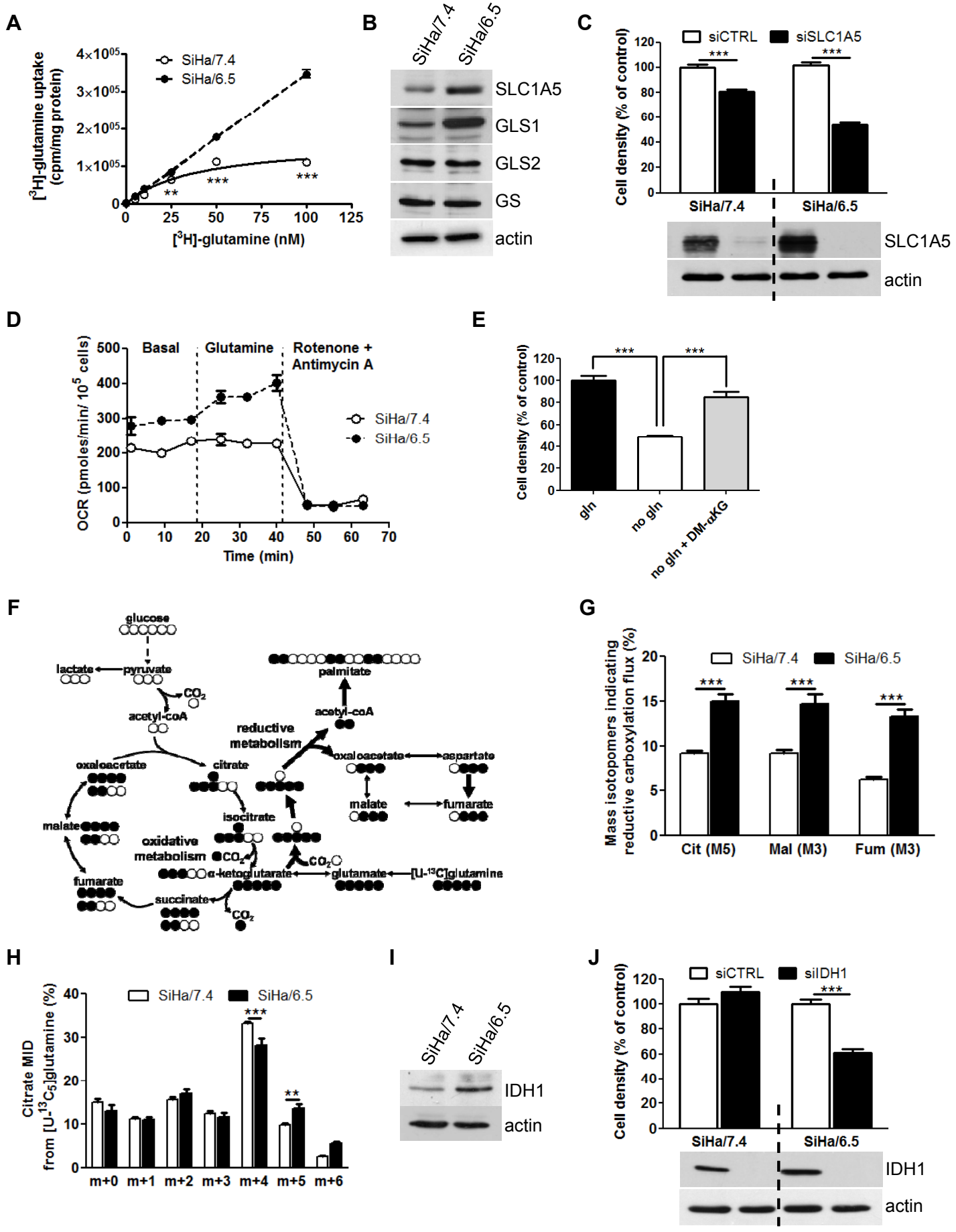

Figure 3

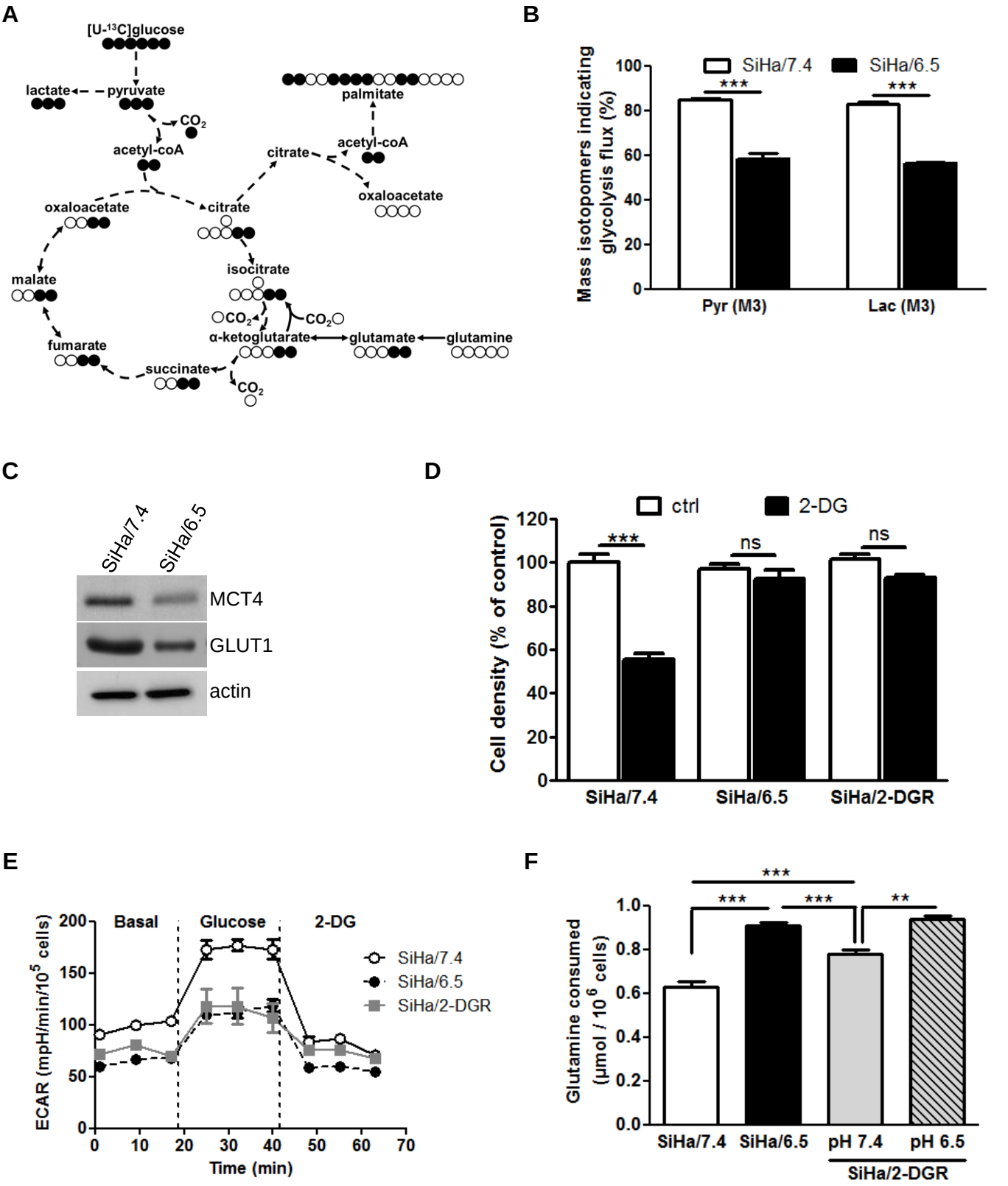

Author Manuscript Published OnlineFirst on August 1, 2014; DOI: 10.1158/0008-5472.CAN-14-0705
Author manuscripts have been peer reviewed and accepted for publication but have not yet been edited.

Figure 4

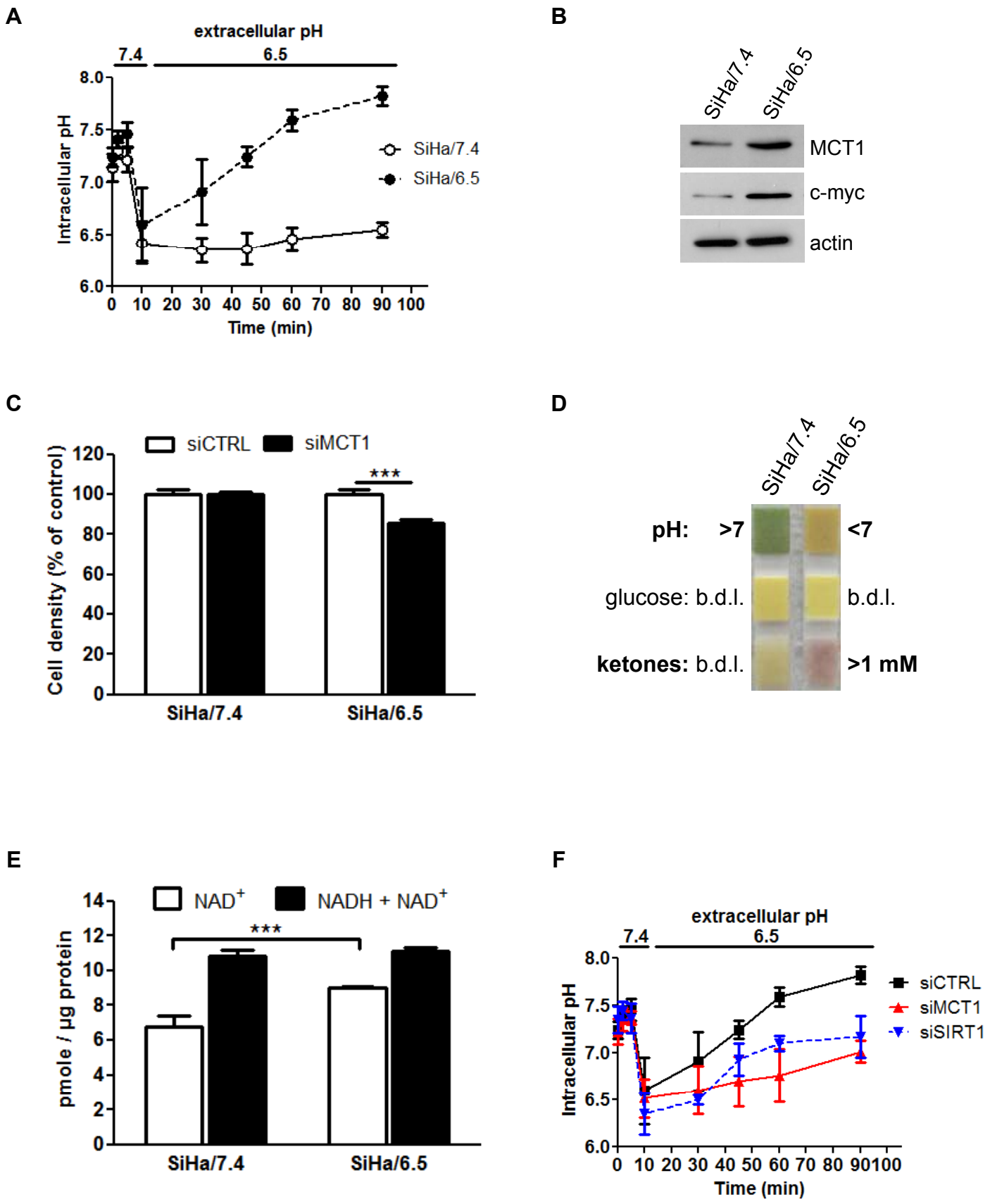

Figure 5

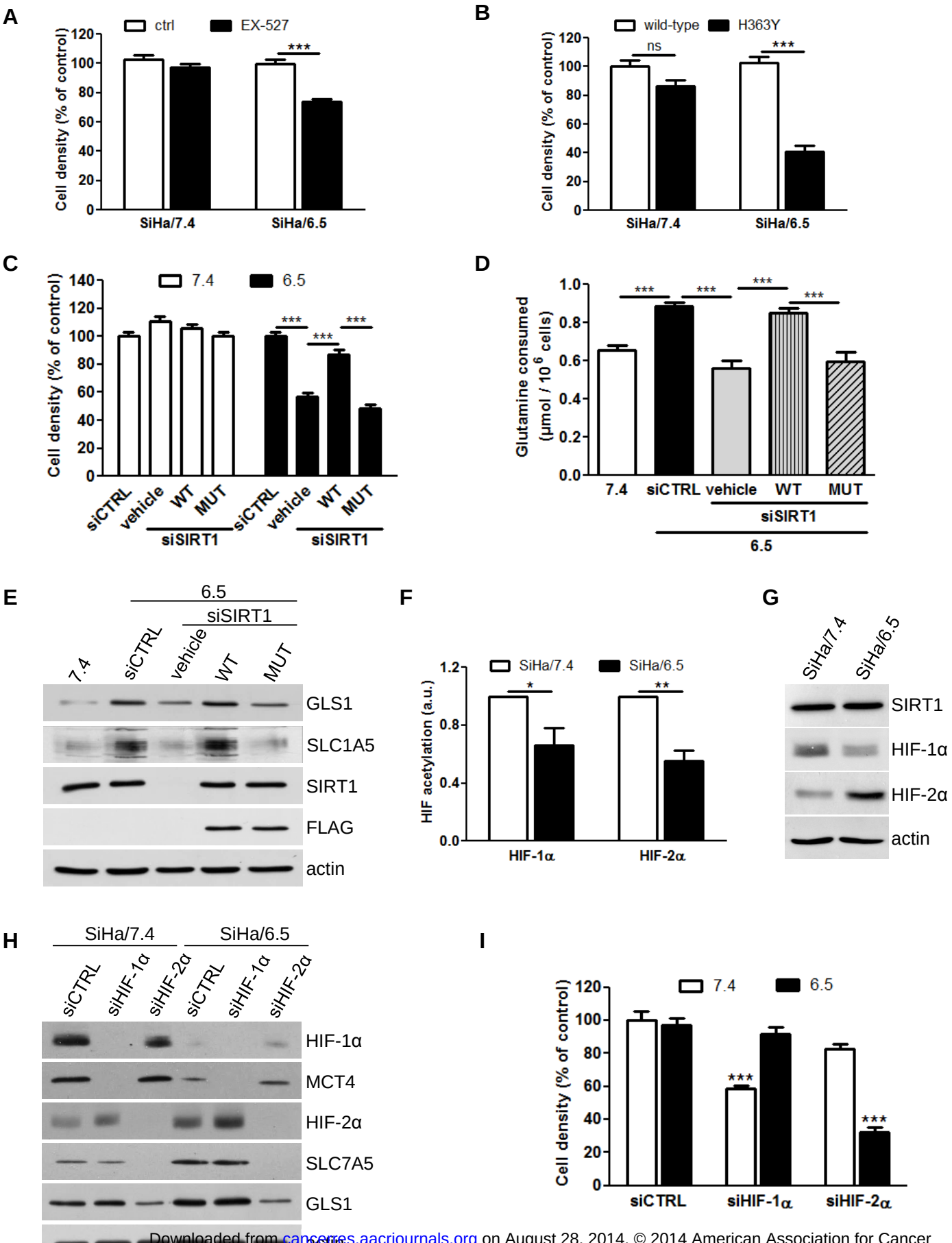

Author Manuscript Published OnlineFirst on August 1, 2014; DOI: 10.1158/0008-5472.CAN-14-0705
Author manuscripts have been peer reviewed and accepted for publication but have not yet been edited.

Figure 6

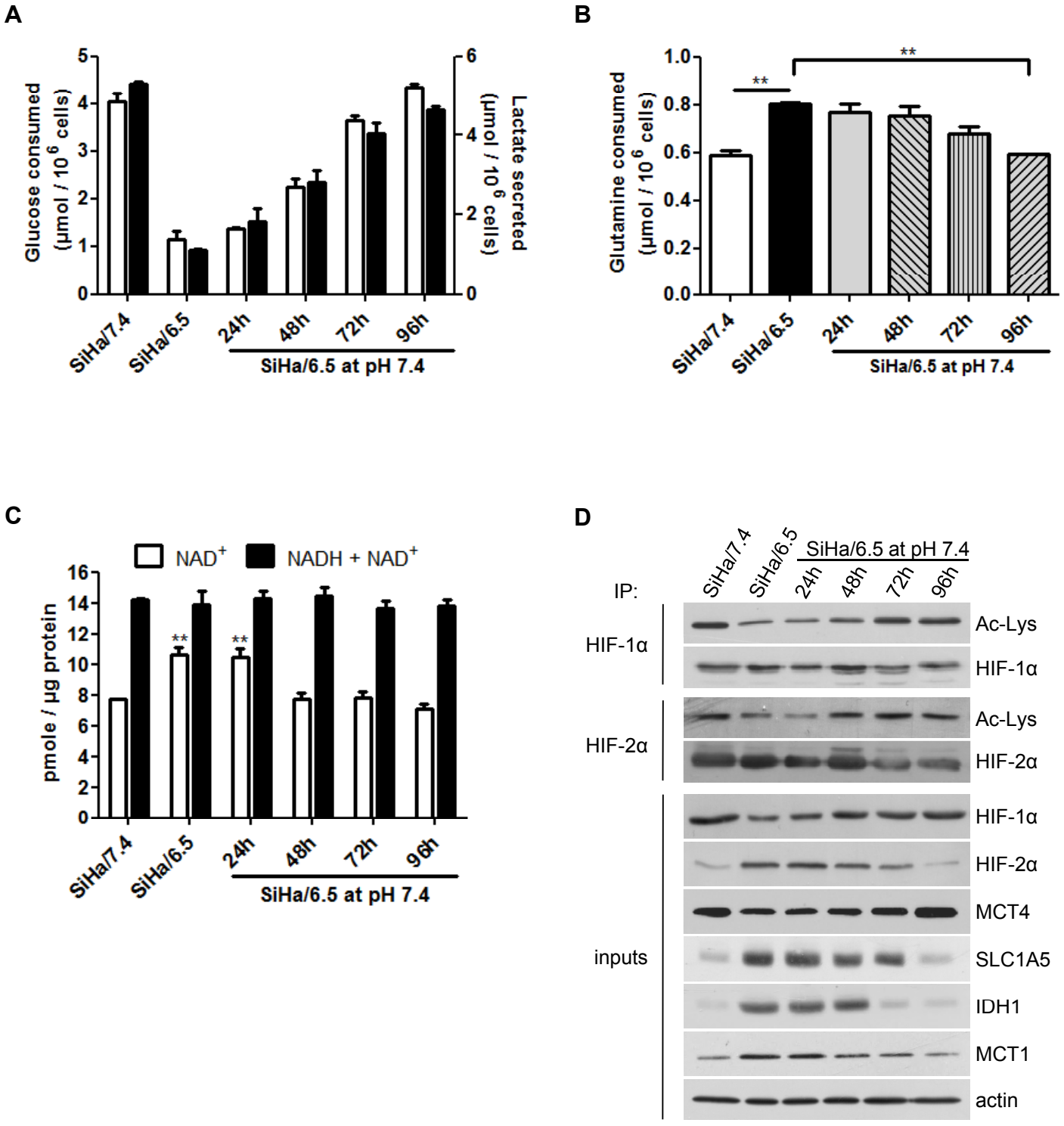

Figure 7